Motion of an Elastic Beam Supporting a Moving Rigid Body

Shlomo Djerassi*
RAFAEL, Ministry of Defense, 31021 Haifa, Israel

Introduction

FIGURE 1 shows a system S consisting of an elastic beam B of length L supporting a moving rigid body C. $\bar{C}$ and $\hat{C}$ are support points fixed in C, and $\bar{P}$ and $\hat{P}$ are points of the neutral axis of B, momentarily in contact with $\bar{C}$ and $\hat{C}$, respectively. C is made to move with respect to B with the aid of an actuator fixed to C at $\hat{C}$. The actuator applies a tangential driving force of magnitude F to B at $\hat{P}$ and to C at $\hat{C}$.

Similar systems are frequently encountered in mechanics. Cranes carrying carts, cannon firing rounds, and printers carrying cartridges are examples. A recent example of interest is the central truss of the International Space Station (ISS) carrying the mobile transporter (MT). In all of these examples, the motion of the rigid body along the beam induces vibrations that could considerably affect the performance of the entire system.

Systems involving sliding motions of elastic bodies were investigated in the past. Examples are the deployment of elastic bodies from rigid bases[1] and motions of elastic beams over fixed supports.[2] To date, only Tadikonda[3] and Bhatta et al.[4] have addressed the problem of two elastic bodies sliding with respect to one another. These authors generated constraint equations, which they imposed on the equations of motion of the unconstrained system. It seems that terms associated with geometric stiffening[5] have not been employed and, hence, that the validity of the indicated works is limited to slow motions.

It is the purpose of this work to study motions of systems of the type in question with the aid of numerical integration of the governing equations, including terms associated with geometric stiffening. To this end, B and C are regarded momentarily as undergoing an unconstrained motion. Motion equations of the unconstrained system are formulated with the aid of the assumed mode method. In addition, constraint equations are formulated and the fact that $\bar{P}$ and $\hat{P}$ are not fixed in B, whereas $\bar{C}$ and $\hat{C}$ are fixed in C, is taken into account. The two sets of equations are combined in conjunction with Kane's equations for constrained systems,[6] producing the requisite equations of motion. The latter are applied to two systems of a different character. One comprises the ISS and its MT in a speedup maneuver and another comprises a cannon barrel and a round in a firing process.

Equations of Motion

Suppose that B and C in Fig. 1 undergo a planar, unconstrained motion, that is, there is no contact between B and C. A reference frame A is defined along with $\boldsymbol{a}_i$, $\boldsymbol{c}_i$, and $\boldsymbol{n}_i$, $i = 1, 2, 3$, three triads of dextral, mutually perpendicular unit vectors fixed in A, C, and N, a Newtonian reference frame, respectively, so that $\boldsymbol{a}_3$, $\boldsymbol{c}_3$, and $\boldsymbol{n}_3$ are normal to the plane of motion. $\bar{B}$ and $\hat{B}$ are the endpoints of B; $\boldsymbol{a}_1$ is aligned with l_A, a line tangent to the neutral axis of B at $\bar{B}$; and $\boldsymbol{c}_1$ is aligned with l_C, a line passing through $\bar{C}$ and $\hat{C}$. Here $q_{\nu+3}$ and $q_{\nu+6}$ are angles measured from $\boldsymbol{n}_1$ to $\boldsymbol{a}_1$ and from $\boldsymbol{n}_1$ to $\boldsymbol{c}_1$ in accordance with the right-hand rule. Furthermore, if P is a generic point of B whose position in A is given by $\boldsymbol{p}^{BP} = \xi\boldsymbol{a}_1 + y(\xi, t)\boldsymbol{a}_2$, then the assumed mode method makes it possible to describe the elastic deformation of B at P as

$$y(\xi, t) = \sum_{j=1}^{\nu} \phi_j(\xi) q_j(t)$$

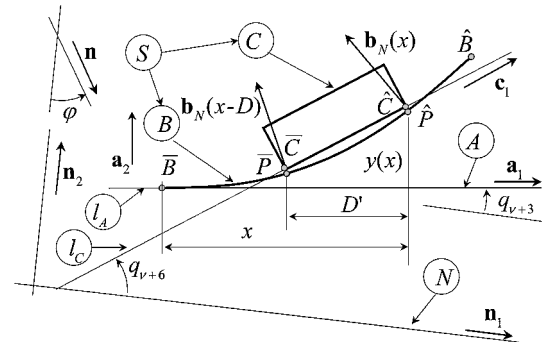

Fig. 1 Rigid body in contact with an elastic beam.

where $\phi_j(\xi)$ is a function of ξ called the jth modal function, q_j is a function of time called the jth modal coordinate, and ν is a number. One may now associate with the unconstrained motion of S in N generalized speeds $u_{\nu+1}, \ldots, u_{\nu+6}$ defined such that

$$\boldsymbol{v}^{\bar{B}} = u_{\nu+1}\boldsymbol{n}_1 + u_{\nu+2}\boldsymbol{n}_2, \qquad \omega^A = u_{\nu+3}\boldsymbol{n}_3 \tag{1}$$

$$\boldsymbol{v}^{\hat{C}} = u_{\nu+4}\boldsymbol{n}_1 + u_{\nu+5}\boldsymbol{n}_2, \qquad \omega^C = u_{\nu+6}\boldsymbol{n}_3 \tag{2}$$

where, for example, $\boldsymbol{v}^{\bar{B}}$ is the velocity of $\bar{B}$ in N and ω^A is the angular velocity of A in N. Accordingly, if C^* is the mass center of C whose position is given by $\boldsymbol{p}^{\hat{C}C^*} = p_1\boldsymbol{c}_1 + p_2\boldsymbol{c}_2$, then the velocities of P and C^* are given by

$$\boldsymbol{v}^P = \left[-\sum_{j=1}^{\nu}\sum_{i=1}^{\nu} \varepsilon_{ji}(\xi) q_i u_j + c_{\nu+3}u_{\nu+1} + s_{\nu+3}u_{\nu+2} - y(\xi)u_{\nu+3} \right]\boldsymbol{a}_1 + \left[\sum_{j=1}^{\nu} \phi_j(\xi)u_j - s_{\nu+3}u_{\nu+1} + c_{\nu+3}u_{\nu+2} + \xi u_{\nu+3} \right]\boldsymbol{a}_2 \tag{3}$$

$$\boldsymbol{v}^{C^*} = u_{\nu+4}\boldsymbol{n}_1 + u_{\nu+5}\boldsymbol{n}_2 - u_{\nu+6}p_2\boldsymbol{c}_1 + u_{\nu+6}p_1\boldsymbol{c}_2 \tag{4}$$

where $c_{\nu+3} = \cos q_{\nu+3}$, $s_{\nu+3} = \sin q_{\nu+3}$, and u_j is the time derivative of q_j, $j = 1, \ldots, \nu$. These expressions are obtained with the aid of Eqs. (1) and (2), respectively. The quantities $\varepsilon_{ji}(\xi)$, $j, i = 1, \ldots, \nu$, are associated with correct linearization of $\boldsymbol{v}^P$ and, in connection with the inextensible Euler–Bernoulli beam, are shown by Buffinton and Kane[2] to equal

$$\varepsilon_{ji}(\xi) = \int_0^{\xi} \phi_j'(\sigma)\phi_i'(\sigma)\,\mathrm{d}\sigma \tag{5}$$

Defining $q_{\nu+1}$ and $q_{\nu+2}$ as the Cartesian coordinates of $\bar{B}$ in N, and $q_{\nu+4}$ and $q_{\nu+5}$ as the Cartesian coordinates of $\hat{P}$ in N, one has $u_r = \dot{q}_r$, $r = \nu+1, \ldots, \nu+6$, where $q_{\nu+3}$ and $q_{\nu+6}$ are the angles defined earlier. These definitions suffice for the generation of generalized inertia forces for B.

Now, the system is subjected to a number of active forces, as follows. First is the driving force $\boldsymbol{F}$ exerted by $\hat{C}$ on $\hat{P}$. This force is defined as $\boldsymbol{F} = f(t)\boldsymbol{b}_T(x)$, where $\boldsymbol{b}_T(x)$ is a unit vector tangent to the neutral axis of B at $\hat{C}$ and is given by

$$\boldsymbol{b}_T(x) = \cos[\bar{y}'(x)]\boldsymbol{a}_1 + \sin[\bar{y}'(x)]\boldsymbol{a}_2 \tag{6}$$

where $\bar{y}'(x) = \tan^{-1}[y'(x)]$ and x is defined as the $\boldsymbol{a}_1$ measure number of $\boldsymbol{p}^{\bar{B}\hat{P}}$, the position vectors from $\bar{B}$ to $\hat{P}$, namely, $\boldsymbol{p}^{\bar{B}\hat{P}} = x\boldsymbol{a}_1 + y(x)\boldsymbol{a}_2$. Second are gravitational forces aligned with a unit vector $\boldsymbol{n}$ defined as $\boldsymbol{n} = \sin(\varphi)\boldsymbol{n}_1 - \cos(\varphi)\boldsymbol{n}_2$, where φ is the angle shown in Fig. 1. Third are elastic forces derivable from the potential function $EJL(q_1^2\lambda_1^4 + \cdots + q_\nu^2\lambda_\nu^4)/2$, where EJ is the bending rigidity of the beam and λ_j is the jth eigenvalue of the characteristic equation of an Euler–Bernoulli beam, chosen to be in a clamped–free configuration (the motion of B in A resembles the motion of a cantilever beam). Fourth are damping forces derivable from the potential

Received 27 April 2000; revision received 5 January 2001; accepted for publication 8 March 2001.

*Research Fellow, P.O. Box 2250.

function $cL(u_1^2+\cdots+u_\nu^2)/2$, where c is the modal damping, assumed to be identical for all modes. These definitions underlie the generation of generalized active forces for B.

Sums of the generalized active force and the generalized inertia force $F_r+F_r^*$, $r=1,\ldots,\nu+3$, for B can now be formed. For $r=1,\ldots,\nu$, they read

$$F_j+F_j^*=-m_B\left[G_j\dot{u}_j-\left(c_{\nu+3}\sum_{i=1}^{\nu}\frac{H_{ji}q_i}{L}+s_{\nu+3}E_j\right)\dot{u}_{\nu+1}-\left(s_{\nu+3}\sum_{i=1}^{\nu}\frac{H_{ji}q_i}{L}-c_{\nu+3}E_j\right)\dot{u}_{\nu+2}+LF_j\dot{u}_{\nu+3}-\left(G_jq_j-\sum_{i=1}^{\nu}J_{ji}q_i\right)u_{\nu+3}^2\right]-EJLq_j\lambda_j^4-cLG_ju_j+F\left[\sum_{i=1}^{\nu}\varepsilon_{ji}(x)q_i-\phi_j(x)y'(x)\right]-m_Bg\left[\cos(\varphi-q_{\nu+3})E_j+\sin(\varphi-q_{\nu+3})\sum_{i=1}^{\nu}\frac{H_{ji}q_i}{L}\right]\qquad(j=1,\ldots,\nu)\tag{7}$$

where m_B is the mass of B and, for $j,i=1,\ldots,\nu$,

$$E_j=\frac{1}{L}\int_0^L\phi_j(\xi)\,\mathrm{d}\xi,\qquad F_j=\frac{1}{L^2}\int_0^L\xi\phi_j(\xi)\,\mathrm{d}\xi$$

$$G_j=\frac{1}{L}\int_0^L\phi_j^2(\xi)\,\mathrm{d}\xi,\qquad H_{ji}=\int_0^L\varepsilon_{ji}(\xi)\,\mathrm{d}\xi$$

$$J_{ji}=\frac{1}{L}\int_0^L\xi\varepsilon_{ji}(\xi)\,\mathrm{d}\xi$$

Note that $\varepsilon_{ji}(x)$, $j,i=1,\ldots,\nu$, appearing in Eqs. (7) are defined as in Eq. (5) with x replacing ξ. Since $\mathrm{d}\varepsilon_{ji}/\mathrm{d}x=\phi_j'(x)\phi_i'(x)$, then

$$\frac{\mathrm{d}\varepsilon(x)_{ji}}{\mathrm{d}t}=\dot{x}\phi_j'(x)\phi_i'(x)\qquad(j,i=1,\ldots,\nu)\tag{8}$$

equations, which can be integrated to produce $\varepsilon_{ji}(x)$, $j,i=1,\ldots,\nu$.

Expressions for $F_r+F_r^*$, $r=\nu+4$, $\nu+5$, $\nu+6$, associated with the motion of C can be formed straightforwardly if use is made of Eqs. (2) and if account is taken of the driving force $\boldsymbol{F}$ and the gravitation force $m_Cg\boldsymbol{n}$. In conclusion, the motion of the unconstrained system is governed by the dynamic equations

$$F_r+F_r^*=0\qquad(r=1,\ldots,\nu+6)\tag{9}$$

and by the kinematic equations

$$\dot{q}_r=u_r\qquad(r=1,\ldots,\nu+6)\tag{10}$$

Constraint Equations

As indicated, C slides along B so that points $\bar{C}$ and $\hat{C}$ of C come momentarily into contact with points $\bar{P}$ and $\hat{P}$ of B. Hence,

$$(\boldsymbol{v}^{\bar{C}}-\boldsymbol{v}^{\bar{P}})\cdot\boldsymbol{b}_N(x-D')=0\tag{11}$$

$$(\boldsymbol{v}^{\hat{C}}-\boldsymbol{v}^{\hat{P}})\cdot\boldsymbol{b}_N(x)=0\tag{12}$$

where, for example, $\boldsymbol{v}^{\bar{C}}$ is the velocity of $\bar{C}$ in N and $\boldsymbol{b}_N(x)$ and $\boldsymbol{b}_N(x-D')$ are unit vectors perpendicular to the neutral axis of B at $\bar{P}$ and $\hat{P}$, respectively, given by

$$\boldsymbol{b}_N(x-D')=-\sin[y'(x-D')]\boldsymbol{a}_1+\cos[y'(x-D')]\boldsymbol{a}_2\tag{13}$$

$$\boldsymbol{b}_N(x)=-\sin[y'(x)]\boldsymbol{a}_1+\cos[y'(x)]\boldsymbol{a}_2\tag{14}$$

where $D'=D\cos(q_{\nu+6}-q_{\nu+3})$ and D is the distance from $\bar{C}$ to $\hat{C}$. Expressions for $\boldsymbol{v}^{\bar{P}}$ and $\boldsymbol{v}^{\hat{P}}$ can be derived from Eq. (3) if ξ is replaced with $x-D$ and x, respectively. Then substitutions in Eqs. (11) and (12) give rise to two relations between generalized speeds, which, when solved for $u_{\nu+5}$ and $u_{\nu+6}$ and linearized in q_r and u_r, $r=1,\ldots,\nu$, and in $[q_{\nu+6}-q_{\nu+3}-y'(x-D')]$ about zero, lead to the following constraint equations:

$$u_{\nu+5}=\left[\sum_{j=1}^{\nu}\phi_j(x)u_j+xu_{\nu+3}\right]\frac{1+t_{\nu+3}y'(x)}{c_{\nu+3}}-\frac{t_{\nu+3}+y'(x)}{c_{\nu+3}^2}(u_{\nu+1}-u_{\nu+4})+u_{\nu+2}\tag{15}$$

$$u_{\nu+6}=\sum_{j=1}^{\nu}\frac{[\phi_j(x)-\phi_j(x-D)]u_j}{D}+\bar{y}''(x)\left[\sum_{j=1}^{\nu}\phi_j(x)u_jt_{\nu+3}-\frac{u_{\nu+1}-u_{\nu+4}}{c_{\nu+3}}-xt_{\nu+3}u_{\nu+3}\right]+u_{\nu+3}\tag{16}$$

where $t_{\nu+3}=\tan q_{\nu+3}$ and $\bar{y}''(x)\hat{=}[y'(x)-y'(x-D)]/D$. D in $y'(x-D)$ replaces D' because the difference between $y'(x-D')$ and $y'(x-D)$ comprises a third-order expression in the modal coordinates. Moreover, the variable x defined earlier is not independent. In fact, its time derivative is given by

$$\dot{x}=(\boldsymbol{v}^{\hat{C}}-\boldsymbol{v}^{\hat{P}})\cdot\boldsymbol{b}_T(x)\tag{17}$$

or, if expressed explicitly,

$$\dot{x}=\sum_{j=1}^{\nu}\sum_{i=1}^{\nu}\varepsilon_{ji}(x)q_iu_j-y'(x)\sum_{j=1}^{\nu}\phi_j(x)u_j-[c_{\nu+3}-s_{\nu+3}y'(x)]\times(u_{\nu+1}-u_{\nu+4})-[s_{\nu+3}+c_{\nu+3}y'(x)]\times(u_{\nu+2}-u_{\nu+5})+[y(x)-xy'(x)]u_{\nu+3}\tag{18}$$

a kinematic equation additional to Eqs. (10). Equations (15) and (16) can be used, in conjunction with Eqs. (9) and Kane's equations for constrained systems[6] to obtain equations governing motions of the constrained system. These were formed and integrated numerically to obtain the following results.

Simulations

ISS and Its MT in a Speedup Maneuver

Thomas and Stubbs[7] developed a continuum equivalent representation of the space station truss. Suppose that, accordingly, a beam with a bending rigidity of $EJ=10^5\ \mathrm{N\cdot m^2}$, a damping coefficient of $c=0.1\ \mathrm{kg-m^{-1}-s^{-1}}$, and mass of 3000 kg represents the truss. Also, suppose that the transporter carrying a load of 1500 kg with a mass center located at $p_1=-5$ and $p_2=7$ m, is initially placed so that $x(0)=L/2$ and is acted on by a driving force of magnitude $F=10$ N for 2 s. Then $\dot{x}$ becomes 0.025 m/s, the maximum transporter speed allowed.[8] In Fig. 2, $y(L,t)$, the elastic deflection of the endpoint $\hat{B}$, is shown for $D=10$ m (thick line). A time behavior indistinguishable from that in Fig. 2 is obtained if the indicated equations are linearized in all of the variables except $u_{\nu+1}$ and $u_{\nu+4}$ and if the terms associated with $\varepsilon_{ji}(x)$, $j,i=1,\ldots,\nu$, are dropped. It can be concluded that analyses such as these in Refs. 3 and 4 can yield satisfactory results even if terms associated with geometrical stiffening are disregarded.

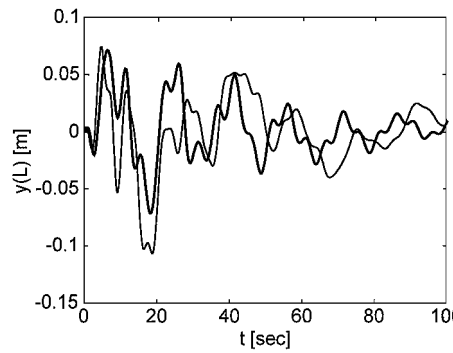

Fig. 2 Truss end deflection during transporter motion.

The thin line in Fig. 2 describes $y(L,t)$ for $D=0.1$ and $p_1=-0.05$ m and shows that the elastic behavior of the beam is only slightly dependent on changes in D. This is also the case if the moment of inertia of the MT is ignored. Thus, meaningful approximations can be obtained if the transporter is assumed to be a particle located at C^*, an assumption that considerably facilitates the analysis.

Cannon Barrel and a Round in a Firing Process

A different state of affairs arises in connection with motions of a cannon firing a round. The barrel is initially deformed due to gravity and is further deformed during the firing process. Moreover, the deformation rate involved is high because the travel time of the round in the barrel is on the order of a few milliseconds. Fire control systems with a typical bandwidth of 20 MHz, which are well suited to deal with the rigid-body motion of the barrel, cannot deal with the elastic deflections in question. However, one can evaluate the deformation and use prefiring corrections, usually referred to as superelevation.[9] The following analysis is directed toward such an evaluation.

Consider a 155-mm Howitzer M198 (Ref. 10) with a 6-m-long barrel. The bending rigidity of the barrel is approximately $EJ=6\times10^5$ N·m^2, and its mass is 380 kg. Suppose that the muzzle speed is 800 m/s. This means that if a round weighs 45 kg a force of magnitude $F=2.4\times10^6$ N is exerted on both the round and the barrel, providing the round with a 5000-g acceleration.

Suppose that a spring of rate k and a damper of rate b represent the recoiling system exerting a force $-(kq_{\nu+1}+bu_{\nu+1})\boldsymbol{a}_1$ on $\bar{B}$ and that a driving force $F\boldsymbol{c}_1$ is exerted on $\hat{C}$ (or equivalently, on $\bar{C}$) and, simultaneously, that a force $-F\boldsymbol{a}_1$ is exerted on $\bar{B}$. Then Eqs. (9), (15), (16), and (18) can be used to simulate the motion of the system (in conjuction with Kane's equations[6] for constrained systems) if Eqs. (9) are slightly modified to account for the recoiling force and the (differently defined) driving force. Also, equations associated with $u_{\nu+2}$ and $u_{\nu+3}$ are discarded, and two additional constraint equations are imposed on the motion, namely, $u_{\nu+2}=0$ and $u_{\nu+3}=0$, and are used to eliminate $u_{\nu+2}$ and $u_{\nu+3}$ and their time derivatives from Eqs. (9), (15), (16), and (18). If Eqs. (9) are linearized in all of the variables except $u_{\nu+1}$ and $u_{\nu+4}$, and if $q_{\nu+3}=0$, they reduce to

$$F_j+F_j^*=-m_B\left[G_j\dot{u}_j-\left(\sum_{i=1}^{\nu}\frac{H_{ji}q_i}{L}\right)\dot{u}_{\nu+1}\right]-EJLq_j\lambda_j^4-cLG_ju_j-m_Bg\left[c\varphi E_j+s\varphi\sum_{i=1}^{\nu}\frac{H_{ji}q_i}{L}\right]\qquad(j=1,\ldots,\nu)\quad(19)$$

$$F_{\nu+1}+F_{\nu+1}^*=-m_B\dot{u}_{\nu+1}-F+m_Bgs\varphi-(kq_{\nu+1}+bu_{\nu+1})\qquad(20)$$

and so on. Moreover, if Eqs. (15), (16), and (18) are linearized similarly, then

$$u_{\nu+5}=\sum_{j=1}^{\nu}\phi_j(x)u_j-y'(x)(u_{\nu+1}-u_{\nu+4})\qquad(21)$$

$$u_{\nu+6}=\sum_{j=1}^{\nu}\frac{[\phi_j(x)-\phi_j(x-D)]u_j}{D}-[y'(x)-y'(x-D)]\frac{u_{\nu+1}-u_{\nu+4}}{D}\qquad(22)$$

$$\dot{x}=-(u_{\nu+1}-u_{\nu+4})\qquad(23)$$

Initially $u_j=\dot{u}_j=0$, $j=1,\ldots,\nu+1$ and $F=0$. Substituting these relations in Eqs. (19) and (20), one obtains

$$-EJLq_j(0)\lambda_j^4-m_Bg\left[c\varphi E_j+s\varphi\sum_{i=1}^{\nu}\frac{H_{ji}q_i(0)}{L}\right]=0\qquad(j=1,\ldots,\nu)\quad(24)$$

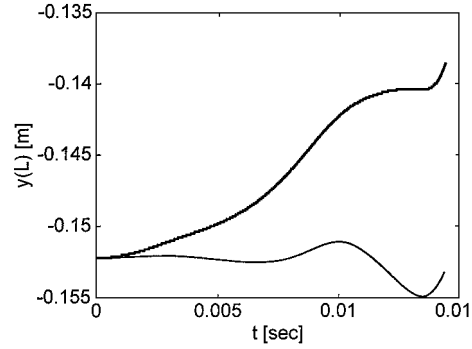

Fig. 3 Barrel end deflection.

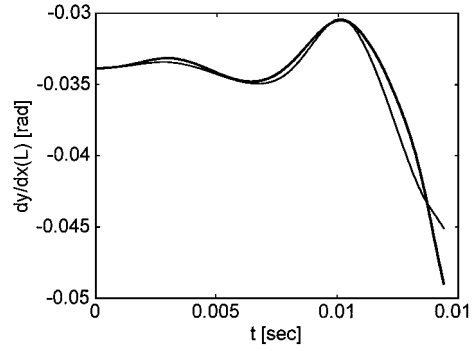

Fig. 4 Barrel end rotation.

$$m_Bgs\varphi-kq_{\nu+1}(0)=0\qquad(25)$$

from which $q_j(0)$, $j=1,\ldots,\nu+1$, and, hence, $y(L,0)$ and $y'(L,0)$ can be deduced. For $D=0.4$, $p_1=-0.25$ and $p_2=0$ m, $k=4\times10^6$ N/m, $b=13{,}000$ N-s/m, $\varphi=-0.5$ rad, and $\nu=6$, Figs. 3 and 4 show $y(L,t)$ and $y'(L,t)$, respectively, obtained with (thick lines) and without (thin lines) the terms associated with $\varepsilon_{ji}(x)$, j, $i=1,\ldots,\nu$. It may be concluded that, although these terms affect the simulation results considerably, they cannot be associated with either the stiffening or softening effects alone. The thick lines in Figs. 3 and 4 seem to indicate first stiffening and then softening of the beam as compared with the stiffness implied by the thin line. Interestingly, it turns out that $\dot{u}_7<0$ and $\ddot{u}_7<0$ throughout the simulated time; hence, u_7 temporal behavior cannot be directly associated with the changes in the apparent barrel stiffness. Figure 4 shows that an elevation correction (superelevation) of 10 mrad can improve the first-round hit probability considerably. Additional runs with smaller D and I_C show that results similar to those shown in Figs. 3 and 4 are obtained. It may be concluded that, as before, the round can be replaced with a particle, facilitating the analysis considerably. It is finally suggested that the $\varepsilon_{ji}(x)$ -associated terms will be called geometric stiffness terms rather geometric stiffening terms.[5] These terms may cause stiffening as well as softening of the structure involved.

Conclusions

The motion of an elastic beam supporting a moving rigid body was investigated with the aid of numerical integration of the governing, partially linearized equations of motion. Two cases were investigated. One case comprises an extremely flexible beam and a slow moving body: Then the geometric stiffness terms in the motion equations can be ignored. Another case comprises a stiff beam and a fast moving body: Then the indicated terms change the dynamic behavior considerably, while causing only slight changes in the apparent stiffness of the beam. In both cases, meaningful results are obtained if the bodies are replaced with particles located at their mass centers.

References

[1] Djerassi, S., "Dynamics of a Satellite Retracting a Long Elastic Appendage," *Journal of Astronautical Sciences*, Vol. 44, No. 4, 1996, pp. 425–442.

[2]Buffinton, K. W., and Kane, T. R., "Dynamics of Beams Moving over Supports," *International Journal of Solids and Structures*, Vol. 21, No. 7, 1985, pp. 617–643.

[3]Tadikonda, S. S. K., "Modeling of Translational Motion Between Two Flexible Bodies Connected via Three Points," *Journal of Guidance, Control, and Dynamics*, Vol. 18, No. 6, 1995, pp. 1392–1397.

[4]Bhatta, M. G., Subramaniam, M., Venngopal, R., and Neguyen, L. H., "Modeling and Simulation of the Mobile Transporter System of International Space Station," *AIAA/USAF/NASA/ISSMO 7th Symposium on Multidisciplinary Analysis and Optimization*, AIAA, Reston, VA, 1998, pp. 1639–1649.

[5]Sharf, I., "Geometric Stiffening in Multibody Dynamics Formulation," *Journal of Guidance, Control, and Dynamics*, Vol. 18, No. 4, 1995, pp. 882–890.

[6]Kane, T. R., and Levinson, D. A., *Dynamics: Theory and Applications*, McGraw–Hill, New York, 1985, p. 158.

[7]Thomas, S., and Stubbs, M., "Dynamic Analysis of the Space Station Truss Structure Based on Continuum Representation," *AIAA/ASME/ASCE/AHS/ASC 30th Conference on Structures, Structural Dynamics, and Materials*, AIAA, Washington, DC, 1989, pp. 1062–1068.

[8]Subramaniam, M., Byun, K. W., and Hua, T., "Control Structure Interaction Analysis of the International Space Station," *AIAA/USAF/NASA/ISSMO 7th Symposium on Multidisciplinary Analysis and Optimization*, AIAA, Reston, VA, 1998, pp. 1628–1638.

[9]Carbonneau, R., Dubois, J., and Harris, G., "An Optical Gun Muzzle Sensor to Improve Firing Accuracy," *Optical Testing and Metrology*, Vol. 661, Society of Photo-Optical Instrumentation Engineers, Bellingham, WA, 1986, pp. 352–358.

[10]*Jane's Armor and Artillery 1995–1996*, edited by C. F. Foss, International Thomson Publ., Surrey, England, U.K., 1996, p. 681.

Near-Optimal Deflection of Earth-Approaching Asteroids

Bruce A. Conway*
University of Illinois at Urbana–Champaign, Urbana, Illinois 61801

Introduction

THE spectacular collision of the Shoemaker-Levy 9 asteroid with Jupiter in July 1994 was a dramatic reminder that the Earth has and will continue to experience catastrophic impact events. Although the frequency of such massive collisions is very low, smaller objects collide with the Earth regularly and do damage that would be intolerable in any populated region. A consensus is developing that, although the probability for collision is low, the potential for destruction is immense and, thus, some resources should be devoted to threat detection and possible interdiction.

The population of known Earth-crossing asteroids is large and continuously increasing by virtue of discovery. As of late 2000, 275 Earth-crossing asteroids (ECAs) that may be termed potentially hazardous are known.[1] For the prevention of a catastrophic impact, the asteroid must be intercepted, at the earliest possible time, and then deflected or destroyed. One strategy may be to detonate a large nuclear weapon at or near the surface of the asteroid or comet, vaporizing part of the surface and yielding an impulsive velocity change because of the momentum imparted to the ejected mass.[2,3]

In a previous Note this author found optimal, that is, minimum time-of-flight, trajectories for the interception of dangerous asteroids.[4] Low-thrust, high specific impulse propulsion was assumed because of the significant advantages it provides in propulsive mass required for a given mission. (An important conclusion of the previous research was that the much greater efficiency of low-thrust electric propulsion would yield a payload mass for the mission of approximately 12% of launch vehicle mass compared with only about 3% using conventional chemical propulsion.)

In this companion Note, the emphasis will be on the process of optimizing the deflection of the dangerous asteroid, at the time of its close approach to Earth, by a given impulse applied at an earlier time. We will again assume that a collision (or near-collision) is imminent, that is, will occur before the asteroid has made another complete revolution about the sun. For most of the known ECAs this means a period of a few years at most to take some type of preventative action.

If the time between application of the deflection impulse and close approach, Δt, is very brief, the deflection $\bar{\Delta}$ can be approximated assuming rectilinear motion, yielding $\bar{\Delta} = (\Delta \bar{v})\ (\Delta t)$ (Ref. 2). The opposite case, in which the asteroid will make more than one orbit of the sun before its close approach to Earth, is an interesting one for which the relationship between the impulse and resulting deflection is much more complicated. Park and Ross show that for this case the best place to apply a deflecting impulse is at asteroid perihelion.[5] Their analysis is one of very few to optimize explicitly the deflecting impulse, for arbitrary Δt, assuming Keplerian motion. However, their solution is two dimensional, that is, it assumes the asteroid orbits the sun in the ecliptic plane. However, 104 of the 275 known potentially hazardous ECAs have inclination greater than 10 deg, and 49 have inclination greater than 20 deg (Ref. 1).

The intention of this work is to show that a near-optimal determination of the direction in which an impulse should be applied to the asteroid, as well as the resulting deflection, can be found without any explicit optimization. The method is easily applied to the true, three-dimensional geometry of the problem.

Maximization of the Deflection

The objective is to determine the direction in which a given impulse should be applied to the asteroid at interception to maximize the subsequent close-approach distance of the asteroid (to the Earth). At the time of interception, t_0, the system state transition matrix $\Phi(t, t_0)$ determines the perturbation in position $\delta\bar{r}$ and velocity $\delta\bar{v}$, which will result at time t due to a perturbation in position and velocity applied at t_0 (Ref. 6), that is,

$$\begin{bmatrix} \delta\bar{r} \\ \delta\bar{v} \end{bmatrix} = \Phi(t, t_0) \begin{bmatrix} \delta\bar{r}_0 \\ \delta\bar{v}_0 \end{bmatrix} = \begin{bmatrix} \tilde{R} & R \\ \tilde{V} & V \end{bmatrix} \begin{bmatrix} \delta\bar{r}_0 \\ \delta\bar{v}_0 \end{bmatrix} \tag{1}$$

Therefore,

$$\delta\bar{r}(t) = [R]\delta\bar{v}_0(t_0) \tag{2}$$

and

$$[R] = (r_0/\mu)(1 - F)\left[(\bar{r} - \bar{r}_0)\bar{v}_0{}^T - (\bar{v} - \bar{v}_0)\bar{r}_0{}^T\right] + (C/\mu)\bar{v}\bar{v}_0^T + G[I]$$

$$F = 1 - (r/p)(1 - \cos\theta), \qquad \cos\theta = \bar{r} \cdot \bar{r}_0/rr_0$$

$$G = (1/\sqrt{\mu})\left[\left(rr_0/\sqrt{p}\right)\sin\theta\right] \tag{3}$$

where p is the orbit semilatus rectum,

$$C = (1/\sqrt{\mu})\left[3U_5 - \chi U_4 - \sqrt{\mu}(t - t_0)U_2\right]$$

$$\chi = \sqrt{a}(E - E_0), \qquad \alpha = 1/\mathrm{a}$$

Here a is the orbit semimajor axis, E is the eccentric anomaly, μ is the gravitational parameter, and $U_1(\chi, \alpha)$, $U_2(\chi, \alpha)$, $U_3(\chi, \alpha)$, $U_4(\chi, \alpha)$, and $U_5(\chi, \alpha)$ are the universal functions.[6]

We want to maximize $|\delta\bar{r}(t_c)| = \max([R]\delta\bar{v}_0)$ where the time of interest t_c is the time of close approach to Earth. Equivalently, we may maximize $\delta\bar{v}_0^T[R]^T[R]\delta\bar{v}_0$. This quadratic form is maximized, for given $|\delta\bar{v}_0|$, if $\delta\bar{v}_0$ is chosen parallel to the eigenvector of $[R]^T[R]$ that is conjugate to the largest eigenvalue of $[R]^T[R]$. This yields the optimal direction for the perturbing velocity impulse $\delta\bar{v}_0$, which will be expressed on the space-fixed basis because this is the basis

Received 13 November 2000; revision received 5 February 2001; accepted for publication 14 April 2001.

*Professor, Department of Aeronautical and Astronautical Engineering, 306 Talbot Laboratory; bconway@uiuc.edu. Associate Fellow AIAA.